



Molecular Crystals and Liquid Crystals

Publication details, including instructions for authors and subscription information:

<http://www.tandfonline.com/loi/gmcl20>

Image Analysis to Study LC Alignment on Nanopatterned Substrates

Hemang J. Shah^a, Michael L. Ermold^a & Adam K. Fontecchio^a

^a Department of Electrical and Computer Engineering, Drexel University, Lebow, Philadelphia, USA

Version of record first published: 31 Aug 2006

To cite this article: Hemang J. Shah, Michael L. Ermold & Adam K. Fontecchio (2005): Image Analysis to Study LC Alignment on Nanopatterned Substrates, *Molecular Crystals and Liquid Crystals*, 438:1, 291/[1855]-302/[1866]

To link to this article: <http://dx.doi.org/10.1080/15421400590955488>

PLEASE SCROLL DOWN FOR ARTICLE

Full terms and conditions of use: <http://www.tandfonline.com/page/terms-and-conditions>

This article may be used for research, teaching, and private study purposes. Any substantial or systematic reproduction, redistribution, reselling, loan, sub-licensing, systematic supply, or distribution in any form to anyone is expressly forbidden.

The publisher does not give any warranty express or implied or make any representation that the contents will be complete or accurate or up to date. The accuracy of any instructions, formulae, and drug doses should be independently verified with primary sources. The publisher shall not be liable

for any loss, actions, claims, proceedings, demand, or costs or damages whatsoever or howsoever caused arising directly or indirectly in connection with or arising out of the use of this material.



Image Analysis to Study LC Alignment on Nanopatterned Substrates

Hemang J. Shah
Michael L. Ermold
Adam K. Fontecchio

Department of Electrical and Computer Engineering,
Drexel University, Lebow, Philadelphia, USA

We have studied patterned substrates to identify liquid crystal alignment. The Polarized Optical Microscope (POM) was used to observe the alignment variations. Image analysis algorithms were developed to enhance the alignment information for POM images. The algorithms were developed to correlate the grayscale intensities in the image to the alignment variations. The resulting resolution of alignment variations is higher than the physical dimensions of the patterns. Using the technique, for 500 nm wide grooves, the alignment variations were observed every 166 nm. Thus, a resolution improvement factor of three is obtained.

Keywords: LC alignment; nanopatterned surfaces

INTRODUCTION

Alignment of liquid crystals (LCs) is an important parameter that regulates the efficiency of LC-based devices. There are different types of alignment schemes observed in devices such as polymer dispersed liquid crystals (PDLC) and LC Displays (LCDs). For LCDs, a polyimide coating on ITO glass is rubbed in predefined directions to get a desired pre-tilt angle for planar alignment. The rubbing mechanism is usually performed by a cotton [1–3] cloth or by the stylus of an AFM [4–7]. Chemical [8–10] treatment of the substrate using lecithin is another technique used to align LCs. Microscopic grooves on the

The authors thank Dr. Christopher Li for the POM, Dr. Jonathan Spanier for AFM Lithography, Dr. N. John DiNardo for AFM, and Dr. Yury Gogotsi for the NanoIndenter.

Address correspondence to Adam K. Fontecchio, Department of Electrical and Computer Engineering, Drexel University, 3141 Chestnut St., Lebow 131, Philadelphia, PA 19104. E-mail: fontecchio@drexel.edu

substrate surface provide the mechanism for planar alignment and direction of the LC molecules. However, there are other theories [11] that argue that the alignment is due to the changes in polyimide chains after rubbing as opposed to the formation of grooves on surface. In our previous work [12], we have shown that nanopatterned substrates influence LC alignment.

The dimensions of the grooves and the optical zoom of the microscope limit the identification of alignment variations, in the case of patterned substrates. Using a $50\times$ microscope objective, in addition to the eye-piece magnification, the smallest feature size that can be resolved is 500 nm. For 500 nm wide grooves, the alignment observed using the POM appears uniform across the length of the groove. However, the grooves formed using most patterning/lithography techniques have surface variations along the boundaries. This will lead to a differential alignment of the LCs at the boundaries relative to the alignment in the bulk. The intensity information associated with the pixels in the POM image can be used to identify these variations. The image analysis algorithm that is developed maps the pixilated intensities to colors represented by a color bar. The mapping leads to a coloring of the original grayscale image. The color variations in the color-mapped image indicate the variations in the LC orientation on the surface. A hue-shift operation on the mapped image will lead to a recoloring of the mapped image. A comparison of the two images, colormapped and hue-shifted, reveals the gradients in regions of uniform alignment. Thus, using the colormapped and hue-shifted images, a detailed analysis of the LC alignment can be obtained. The algorithm improves the resolution of alignment variations by a factor of three implying that alignment variations are observed between distances a third of the actual groove width.

METHOD

PMMA and polycarbonate were the substrates for developing patterns and observing the LC alignment. Manufacturing an optically efficient device using patterned polymer and LC requires the matching of polymer and LC ordinary refractive indices. The refractive indices of PMMA and polycarbonate are 1.48 and 1.58 respectively. The LC used was K15 (5CB) which has its ordinary refractive index $n_o \sim 1.5$ and the extra-ordinary refractive index $n_e \sim 1.73$. The AFM was used to characterize materials for surface roughness (~ 5 nm) and presence of any defects before patterning. Because these polymers are free from chemicals that impart homeotropic alignment to LCs, we have assumed planar alignment of the LCs.

The PMMA was patterned using a MTS Nanoindenter using a Berkovich tip (radius ~ 100 nm). The MTS NanoIndenter was operated in the scratch mode to develop the patterns on PMMA. The feature sizes that were obtained are 500 nm (length) \times 500 nm (width) \times 100 nm (depth). The NanoIndenter was programmed to generate intersecting arrays of vertical and horizontal scratches. The pile-up height and scratch width were the parameters used to determine the position of each individual scratch such that pile overlap is avoided. The scratch velocities used were in the range of 25 – 35 $\mu\text{m}/\text{sec}$ at a load of 1 mN. Figure 1 shows the schematic of the patterned PMMA and Figure 2 shows the AFM image of the patterned substrate.

The LC was deposited on the patterned PMMA and the alignment variations were observed under a Polarized Optical Microscope (POM). It can be observed that the LC alignment in grooves and grids is not identical due to the nature of the confinement imparted by the pattern [12]. The alignment variations between different patterns were observed using the light intensity in the POM images. The light intensity varied for grooves patterned at different angles to the horizontal. The results of the alignment variation have been reported in [12].

The intensity of light in the focal plane of the optical microscope is a function of the LC orientation on the surface and the phase retardation of the incident polarized beam. Using the Jones Matrix theory

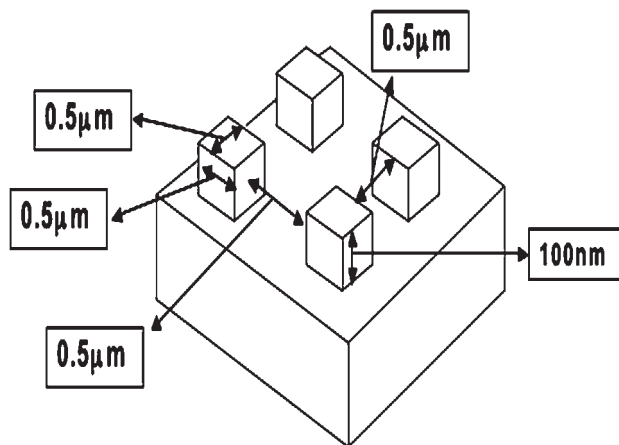


FIGURE 1 Schematic of the patterned substrate.

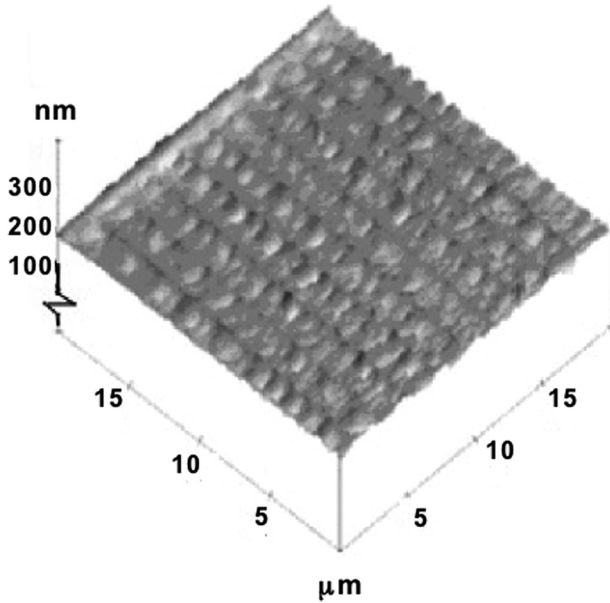


FIGURE 2 3D Atomic Force Micrograph of the nano-patterned PMMA.

described for displays by Yeh and Gu [13], the transmitted intensity of light coming out of the analyzer can be written as:

$$\begin{aligned}
 T = & \cos^2(\phi - \phi_{exit} - \phi_{ent}) + \sin^2 X \sin 2(\phi - \phi_{exit}) \sin 2\phi_{ent} \\
 & + \frac{\phi}{2X} \sin 2X \sin 2(\phi - \phi_{exit} + \phi_{ent}) \\
 & - \phi^2 \frac{\sin^2 X}{X^2} \cos 2(\phi - \phi_{exit}) \cos 2\phi_{ent}
 \end{aligned} \quad (1)$$

In Eq. (1), ϕ represents the twist angle or the orientation angle of the LC, ϕ_{ent} and ϕ_{exit} are the angles of the plane of polarization of the input and output beams, respectively.

$$X = \sqrt{\phi^2 + \left(\frac{\Gamma}{2}\right)^2}$$

where Γ is the phase retardation, and is defined as

$$\Gamma = 2\pi(n_e - n_o)d/\lambda$$

d is the thickness of the LC layer is, and λ is the wavelength of light. For 5CB, n_e is ~ 1.73 and n_o is ~ 1.5 .

The orientation angle is the major parameter that varies in equation 1 signifying that the intensity is mainly dependent on the orientation angle of the LC on the substrate. Thus, the intensity of the light can be used to evaluate the orientation of LCs on the surface.

In case of confined geometries, the sidewalls influence the LC alignment along the groove direction. At the intersection of two or more grooves, referred to herein as “wells”, the LCs lose the alignment acquired outside the area of intersection. The alignment on the surface outside the grooves will be mostly random, dictated by the surface roughness of the material.

We have compared the alignment of LC on the grid with the alignment in grooves patterned at different angles. The schematic of the patterned PMMA substrate is shown in Figure 3a. In Figure 3a, there are grooves along the horizontal, the vertical, at 45-degree and at 60-degree angles to the horizontal. The 60-degree grooves were made to intersect the grid region. LC was deposited on this patterned substrate and the alignment in each groove was examined. Figures 3b and 3c show the patterned substrate before and after LC deposition respectively. Referring Figure 3c, it is observed that the intensity varies between the patterned regions thus signifying different orientation angles for the LC.

We used the AFM in lithography mode for patterning grooves on polycarbonate. The grooves measure 500 nm in width and 50 nm in depth. The patterns developed are shown in Figure 4. LC deposition on these patterns gave the same results as discussed above i.e. the alignment in the confined geometries is different compared to the alignment in the bulk, unpatterned region. Thus, the LC alignment observed in patterns formed using the two techniques is due to the mechanical deformation of the substrate. Figure 5 shows the alignment variation of LC on the AFM patterned polycarbonate. LC was deposited on the patterned polycarbonate and alignment was observed at different polarizer angles as indicated in Figure 5.

IMAGE ANALYSIS

The alignment variation of the LCs in the patterned regions is studied by analysis of POM images. The patterns show feature variations of the order of few nanometers along them due to vibrations during indentation, and the positioning and repositioning of the indenter tip. As a result, the LC alignment will vary across the length of a groove. The imperfect surface of each groove will also lead the alignment at the

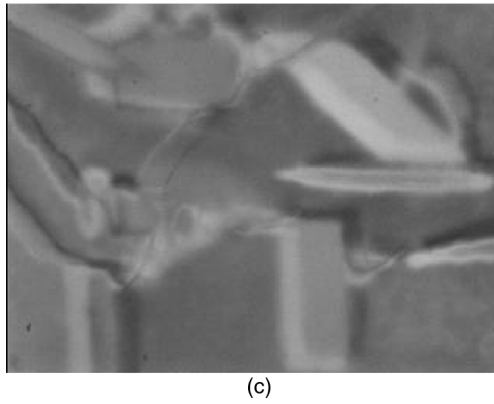
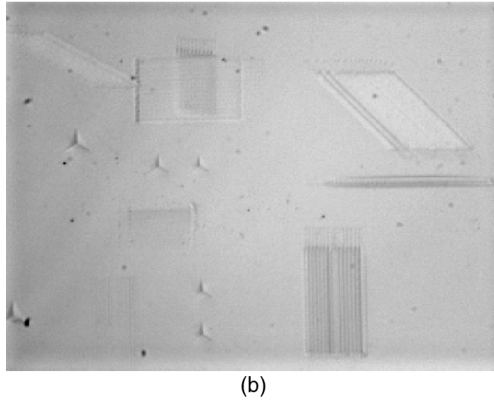
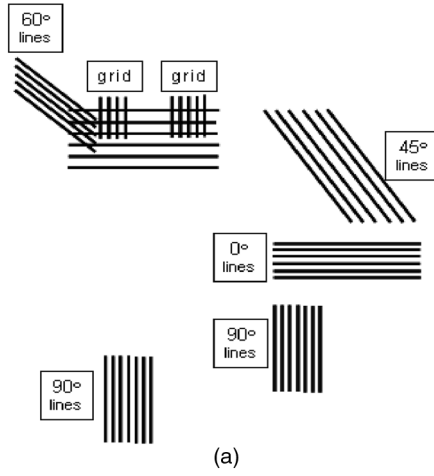


FIGURE 3 POM images of the LC alignment within the patterned substrate. (a) Desired positioning and shape of patterns, (b) Image of the patterned substrate without deposition of LC, and (c) The substrate after LC deposition.

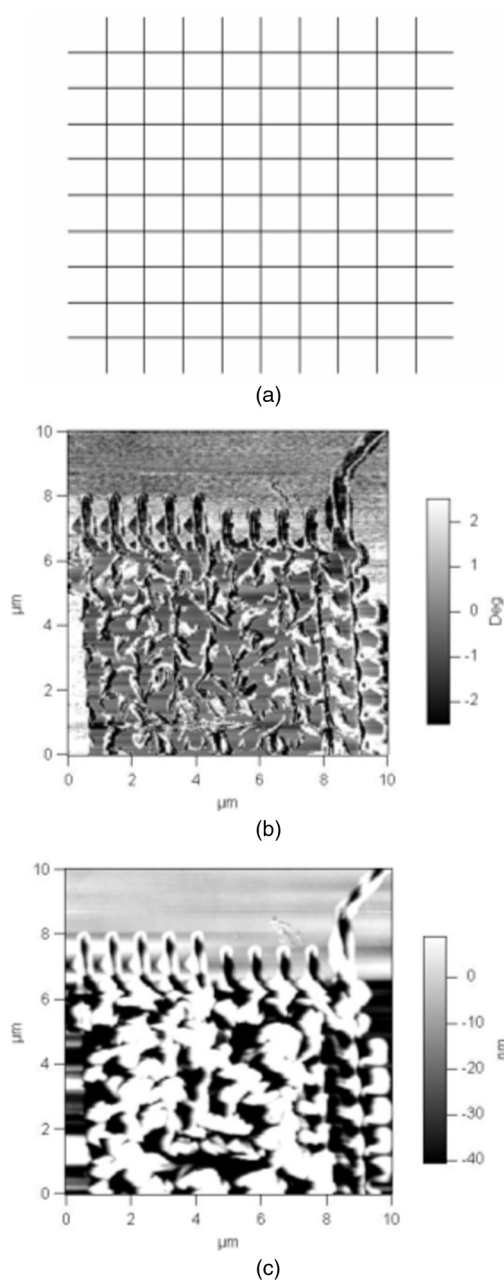
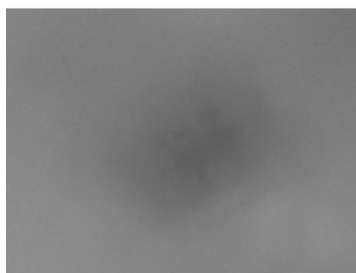


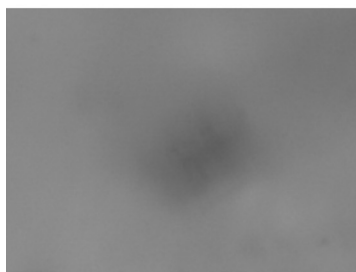
FIGURE 4 AFM lithography. (a) Intended schematic, (b) Phase view of the patterned groove and (c) Height trace of the patterned groove.



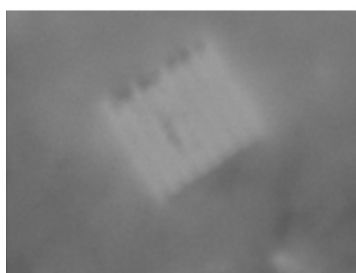
(a)



(b)



(c)



(d)

FIGURE 5 POM images of LC alignment in grooves patterned with AFM on polycarbonate. (a) Polarizer angle = 0° , (b) Polarizer angle = 45° , (c) Polarizer angle = 90° , and (d) Polarizer angle = 135° .

surface to be different than the alignment in the bulk of the groove. In the images, this is observed as variations of the pixilated intensity values at the boundary from those in the bulk of the groove.

This alignment variation is studied by mapping the intensity associated with each pixel of the POM image to a color. The program to map the pixel intensities to color map is implemented in MATLAB[®] (MathWorks, Inc.), using its image processing functions. The first step is a morphological operation on the POM image which divides image into different objects of a fixed size. The image-processing module, including colormapping and hue-shift operation, uses the intensity associated with every object. For the mapping, the objects chosen were disks with a radius of one pixel. The size of the object can be varied as well as other object shapes can be selected. However, the results obtained due to the change in object parameters are inferior. The grayscale intensities of every pixel are mapped to a color bar. In this case, the image data is scaled to the full range of the color map. The identification of gradients in the color-mapped image will identify the LC alignment variations. Thus, complete information regarding alignment variations can be obtained by first applying the color mapping algorithm followed by the identification of gradients. A hue-shift operation, using MATLAB functions, was implemented on the color-mapped image to identify the gradients. The hue-shift operation does not imply a 2D gradient-step operation. The gradients are identified by a pictorial comparison of the color-mapped and hue-shifted images. The gradients correspond to the alignment variations within a pattern. The hue-shift operation is implemented using MATLAB functions that vary the hue components of every pixel as per their defined algorithms. The results of this operation are shown in Figure 6. Comparing 6b. and 6c., we can see that the variations in the alignment within each pattern are highlighted after performing the hue-shift operation on 6b.

The discussed MATLAB algorithms are also applied to the AFM lithographed images. The resulting images for LC alignment in patterned grooves are shown in Figure 7. In this case also, the intensity variations as shown in Figure 7b are clearer after the hue-shift operation. For the grid patterned using the AFM, the images are shown in Figures 7d–f.

The image analysis technique discussed identifies variations between individual objects, which are disks in the algorithm implemented. This implies that the variations can be identified within length-scales of two individual pixels as the disks have a radius of 1 pixel. A groove, which measures 500 nm on the POM image, contained approximately 6 pixels. This implies that the identification of features

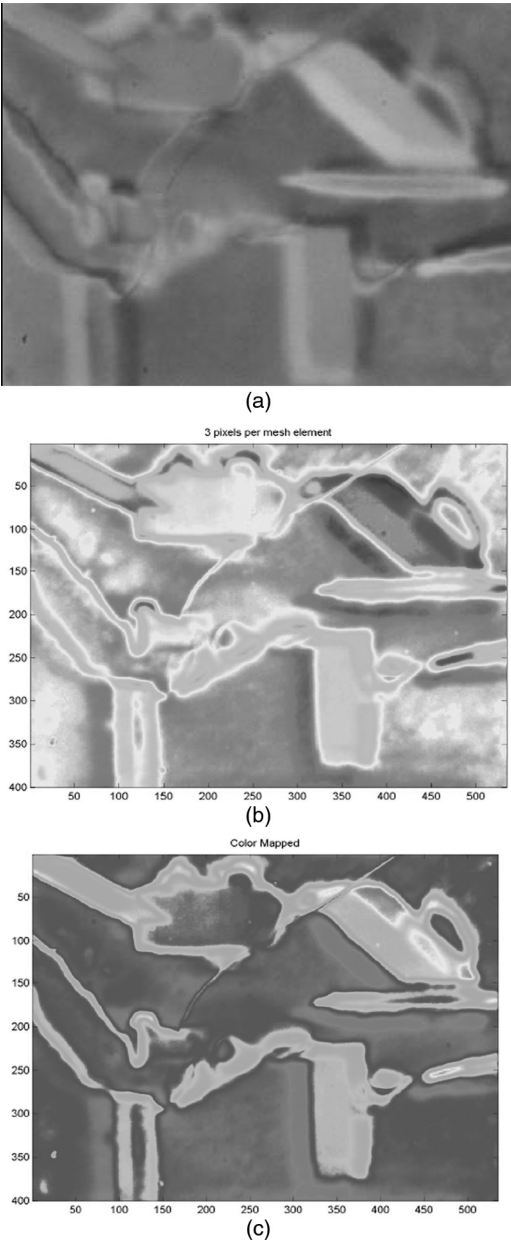


FIGURE 6 (a) POM of LC on patterned PMMA (using Nanoindenter), (b) Color mapped pixilated intensities of 6a. and (c) Hue-shift analysis of 6b.

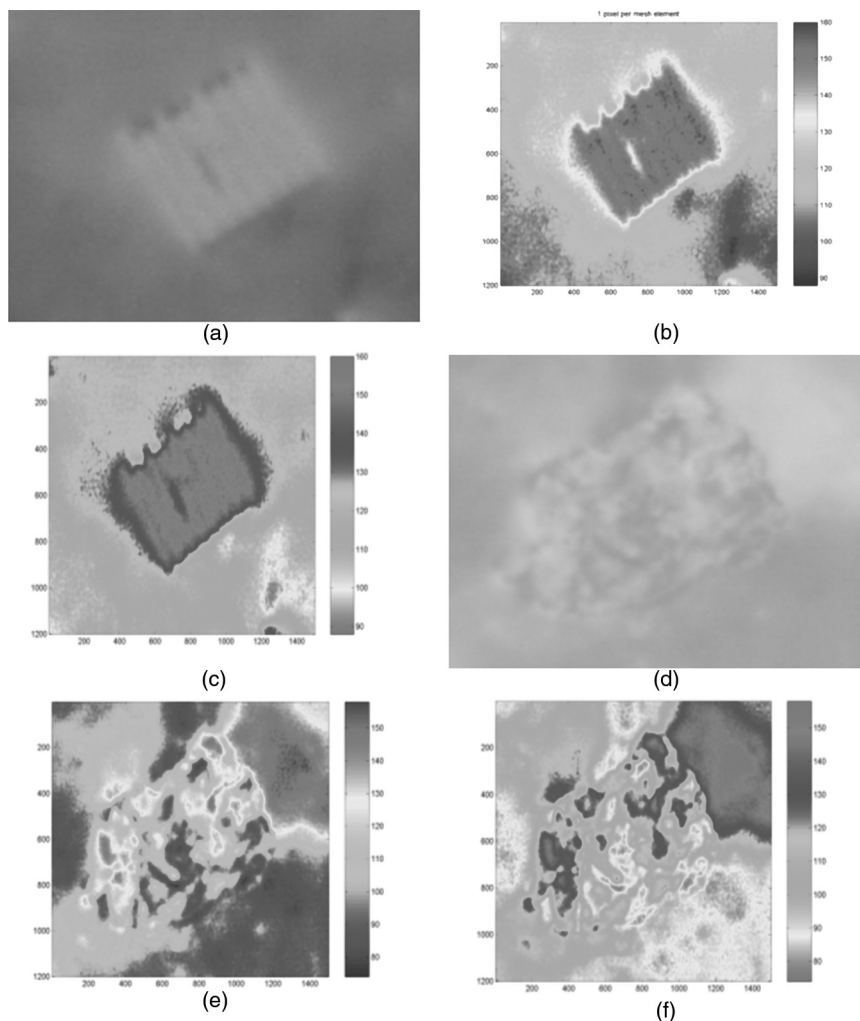


FIGURE 7 (a) and (e) LC on patterned grooves and grid respectively on Polycarbonate (AFM Lithography), (b) and (c) Color mapped pixelated intensities of 7a and 7d, and (d) and (f) Hue-shift of 7b and 7e.

is possible within a length range of ~ 166 nm. As a result, the effective resolution is increased by three times using our technique. This is dependent on the image obtained from the microscope. Higher resolution images will provide better identification of microscopic liquid crystal features.

CONCLUSION

It is shown that the LC alignment induced by nanopatterned substrates has been studied using image analysis of the POM images. The pixilated intensities of the images are color mapped which is followed by a hue-shift operation on the color-mapped image. Thus, the alignment variations of the LC within each pattern can be easily observed. The resolution of identification for variations in alignment was improved by a factor of two pixels, which translated into a resolution of one-third of the feature sizes considered. Thus, variations in alignment of the LCs in patterns can be studied at a higher resolution.

REFERENCES

- [1] Chatelain, P. P. (1943). *Bull. Soc., Franc. Mineral*, 66, 105.
- [2] Berreman, D. W. (1972). *Phys. Rev. Lett.*, 28, 1683.
- [3] Berreman, D. W. (1973). *Mol. Cryst. Liq. Cryst.*, 23, 215.
- [4] Ruetschi, M. Grutter, P. Funschilling, J., & Guntherodt, H.-J. (1994). *Science*, 265, 512.
- [5] Pidduck, J., Haslam, S. D., Bryan-Brown, G. P., Bannister, R., & Kitely, I. D. (1997). *Appl. Phys. Lett.*, 71, 2907.
- [6] Jong-Hyun Kim, Makoto Yoneya, Jun Yamamoto, & Hiroshi Yokoyama, (2001). *Appl. Phys. Lett.*, 78, 3055.
- [7] Bing Wen & Rosenblatt, C. (2001). *J. Appl. Phys.*, 89, 4747.
- [8] Dubois, J. C. et al. (1976). *J. Appl. Phys.*, 47, 1270.
- [9] Janning, J. L. (1972). *Appl. Phys. Lett.*, 21, 173.
- [10] Proust, J. E. et al. (1972). *Solid State Commun.*, 11, 1227.
- [11] Geary, J. M., Goodby, J. W., Kmetz, A. R., & Patel, J. S. (1987). *J. Appl. Phys.*, 62, 4100.
- [12] Shah, H. J. & Fontecchio, A. K. (2003). "Nano-patterned polymer structures for H-PDLCs" SPIE's 48th Annual Meeting, Physical Chemistry and Interfaces II.
- [13] Yeh, P. & Gu. C. (1999). "Optics of Liquid Crystal Displays" Wiley Interscience Publications: New York.
- [14] Shah, H. J., Selinger, R. L. B., Fuller Jr. E. R., & Fontecchio, A. K. (2004). "Modeling of nematic liquid crystal alignment on patterned substrates", submitted at 20th International Liquid Crystals Conference.